JOINT RECOVERY OF UNDER SAMPLED SIGNALS ON A MANIFOLD: APPLICATION TO FREE BREATHING CARDIAC MRI

Sunrita Poddar, Sajan Goud Lingala, Mathews Jacob

University of Iowa, IA, USA

ABSTRACT

We introduce novel algorithms for the joint recovery of an ensemble of signals that live on a smooth manifold from their under sampled measurements. Unlike current methods that are designed to recover a single signal assuming perfect knowledge of the manifold model, the proposed algorithms exploit similarity between the signals without prior knowledge of the underlying manifold structure. Our first algorithm is a two-step scheme, where the Laplacian of the graph associated with the manifold is estimated from similar under sampled measurements made on the signals; this Laplacian is used to formulate the problem as a penalized optimization scheme, where smoothness of the signals on the manifold is chosen as the penalty. The second algorithm is an iterative scheme that alternates between computation of the Laplacian and the signals. Validation of the proposed algorithms using simulations and experimental MRI data demonstrate their utility in accelerating free breathing cardiac MRI.

Index Terms— cardiac MRI, manifolds, compressive sensing, cine, free breathing

1. INTRODUCTION

We consider the joint recovery of an ensemble of high dimensional signals that live on a smooth low dimensional manifold from their under-sampled measurements. Such manifold signal models are appropriate when the signals vary smoothly as a function of a few parameters. Since the dimension of the manifold is often much lower than the ambient dimension, this representation is compact. Our main focus is to exploit the smoothness of the signals on the manifold to make their recovery from under sampled data well-posed.

The main motivation behind this work is the joint reconstruction of a free breathing cardiac image series from MRI data. It is impossible to fully sample each image due to the slow nature of MR acquisitions. The rapid shape changes of the myocardium as a function of time makes it difficult to pose the problem as a temporal smoothness regularized optimization scheme; temporal smoothing will result in extensive blurring of myocardial borders. Each image in the time series is completely characterized by two free parameters—cardiac phase and respiratory phase. If the phases at each time instant can be measured, the Fourier data can be appropriately binned to recover the images. However, the direct measurement of the physiological signals is challenging in many cases due to the interference between the image acquisition scheme and the acquisition of the physiological signals. Recent self navigation strategies that extract cardiac and respiratory phases from the temporal variations of the central Fourier sample (d.c term) are attractive alternatives [1]. However, the utility of these schemes are heavily dependent on the coil geometry and location and the orientation of the slices.

We propose to recover the images lying on a manifold from under sampled measurements. This approach may be viewed as a generalization of the self navigation strategies [1] since knowledge about the manifold structure is recovered from Fourier measurements. This approach relies on the isometry of the cardiac and respiratory phases to the images, which is generally true in cardio-pulmonary imaging.We formulate the joint recovery of the images that live on the manifold as a smoothness regularized optimization scheme, where the regularization penalty is the integral of the square of the gradient magnitude on the manifold. The discretization of this penalty provides a weighted linear combination of image differences, where the weights are non-linear functions of local distances between points. Recent results on compressive manifold embedding guarantee the accurate recovery of local distances from their under sampled Gaussian measurements, provided the number of measurements are greater than a lower bound that is dependent on the dimension of the manifold [2]. Based on these findings, we propose two algorithms for the recovery of the weights and the signals. The first approach is a two step scheme, where the local distances are estimated from under-sampled measurements acquired using the same sampling matrix. These distances are used to define the graph Laplacian, which is used to jointly recover the images. The second algorithm is essentially an iterative refinement of the two-step strategy, where the graph Laplacian is re-computed from the image estimates and is used to specify the criterion at the next iteration. We show that this iterative approach is essentially a majorize-minimize algorithm to solve a smoothness penalized optimization scheme, where the smoothness penalty is computed using a robust scheme.

Most of the current manifold schemes focus on the re-

This work is supported by grants NSF CCF-0844812, NSF CCF-1116067, NIH 1R21HL109710-01A1, and ACS RSG-11-267-01-CCE.

covery of a single signal on the manifold, assuming perfect knowledge of the manifold [2]. In contrast to these schemes, we do not make any assumptions on prior knowledge of the manifold; the structure of the manifold in our setting is heavily dependent on the respiration pattern, as well as cardiac and respiration rate. Our approach is conceptually similar to the non-local schemes in [3], where the manifold structure of image patches are exploited. However, in the patch setting, each of the measurements is a linear combination of all of the signals on the manifold; it is difficult to use the theoretical tools in [2] in this setting. We consider the recovery of several signals, each of which are sampled independently. We validate the proposed algorithm on free breathing cardiac CINE data. The proposed algorithm provided high quality reconstructions with minimal artifacts. These results show that there is a strong isometry between the phases and images.

2. PROBLEM FORMULATION

We consider the recovery of signals $\mathbf{x}_1, \mathbf{x}_2, \ldots \mathbf{x}_k \in \mathcal{M} \subseteq \mathbb{R}^N$ where $\mathcal{M}$ is a smooth *m*-dimensional manifold isometric to the parameter space: $\boldsymbol{\Theta} \subseteq \mathbb{R}^m$ ($m << N$). Specifically, we assume that there exists $\boldsymbol{\theta}_1, \boldsymbol{\theta}_2, \ldots, \boldsymbol{\theta}_n \in \mathbb{R}^m$ such that $\|\mathbf{x}_i - \mathbf{x}_j\| \propto \|\boldsymbol{\theta}_i - \boldsymbol{\theta}_j\|$. In our setting $\boldsymbol{\theta}_i$ is a 2-D vector whose elements are the cardiac and respiratory phases, and $\mathbf{x}_i$ is the image corresponding to these phases. We have the under-sampled measurements:

$$\mathbf{y}_i = \mathbf{A}_i \mathbf{x}_i + \boldsymbol{\eta}_i. \tag{1}$$

Here, $\mathbf{A}_i \in \mathbb{R}^M \times \mathbb{R}^N; M < N$ is the linear measurement operator for the i^{th} image and $\boldsymbol{\eta}_i$ is the noise vector. Since the measurement operators are under-determined, the direct recovery of $\mathbf{x}_i$ from their measurements is ill-posed.

The smoothness of the signals that live on the manifold can be exploited by posing their recovery from their measurements $\mathbf{y}$ as a Tikhonov regularized reconstruction scheme:

$$\{\mathbf{x}^*\} = \arg\min_{\mathbf{x}} \|\mathcal{A}(\mathbf{x}) - \mathbf{y}\|^2 + \lambda \underbrace{\int_{\mathcal{M}} \|\nabla_{\mathcal{M}} \mathbf{x}\|^2 d\mathcal{M}}_{\int_{\mathcal{M}} \mathbf{x}\, \Delta_{\mathcal{M}}\, \mathbf{x}\, d\mathcal{M}} \tag{2}$$

Here, $\nabla_{\mathcal{M}}$ and $\Delta_{\mathcal{M}}$ are the gradient on $\mathcal{M}$ and the Laplace-Beltrami operator, respectively. Since we only have samples $\mathbf{x}_i$ on the manifold, we discretize the above problem as

$$\{\mathbf{x}_i^*\} = \arg\min_{\mathbf{x}_i} \sum_{i=1}^{k} \|\mathbf{A}_i \mathbf{x}_i - \mathbf{y}_i\|^2 + \lambda\, \mathbf{X}^T \mathbf{L} \mathbf{X}. \tag{3}$$

Here $\mathbf{X} = \begin{bmatrix} \mathbf{x}_1^T & \mathbf{x}_2^T & \ldots & \mathbf{x}_k^T \end{bmatrix}^T$ and $\mathbf{L}$ is the Laplacian of the associated graph, specified by $\mathbf{L} = \mathbf{D} - \mathbf{W}$. Here,

$$\mathbf{W}_{i,j} = \varphi_\sigma \left(\|\boldsymbol{\theta}_i - \boldsymbol{\theta}_j\| \right), \tag{4}$$

where φ is an appropriately chosen localized non-linear function. $\mathbf{D}$ is the diagonal matrix, whose diagonals are specified by $\mathbf{D}_{i,i} = \sum_j \mathbf{W}_{i,j}$. If the parameter vector (e.g. cardiac and respiratory phases) corresponding to each image is known, $\mathbf{L}$ can be computed.

2.1. Two-step manifold unaware recovery

As described earlier, it is often difficult to directly measure the underlying parameter $\boldsymbol{\theta}$ along with the signal; it is desirable to estimate the parameter—or equivalently $\mathbf{W}$ from the measured data itself. Wakin [2], has recently shown that under weak conditions, the measurement of the signal samples by the $M \times N$ Gaussian random matrix $\boldsymbol{\Phi}$, specified by $\mathbf{y}_i = \boldsymbol{\Phi}\mathbf{x}_i$ preserves distances:

$$(1-\epsilon)\|\mathbf{x}_i - \mathbf{x}_j\| \leq \|\boldsymbol{\Phi}\mathbf{x}_j - \boldsymbol{\Phi}\mathbf{x}_j\| \leq (1+\epsilon)\|\mathbf{x}_i - \mathbf{x}_j\|, \tag{5}$$

provided $M \geq 18\epsilon^{-2}\, f(m)$, where $f(m)$ is a non-linear function that is dependent on the dimension of the manifold m rather than the ambient dimension N. Note that the measurement matrix $\boldsymbol{\Phi}$ is assumed to be the same for all the signals $\mathbf{x}_i; i = 1, .., k$. Since we assume the manifold to be isometric to the parameters (i.e., $\|\mathbf{x}_i - \mathbf{x}_j\| \propto \|\boldsymbol{\theta}_i - \boldsymbol{\theta}_j\|$), we propose to approximate (4) as

$$\mathbf{W}_{i,j} = \varphi_{\sigma'} \left(\|\boldsymbol{\Phi}\mathbf{x}_i - \boldsymbol{\Phi}\mathbf{x}_j\| \right), \tag{6}$$

where σ' is chosen appropriately.

Our final goal is to recover the images from their under sampled measurements. While the same sampling pattern needs to be used for all images to recover the weights as in (6), this is not beneficial for the reconstruction of images using (3). If the same pattern is used every frame, there is little value in exploiting the similarity beyond noise reduction. Hence, we propose to use the sampling scheme

$$\mathbf{y}_i = \underbrace{\begin{bmatrix} \boldsymbol{\Phi} \\ \mathbf{B}_i \end{bmatrix}}_{\mathbf{A}_i} \mathbf{x}_i + \boldsymbol{\eta}_i, \tag{7}$$

where we fix $\boldsymbol{\Phi}$ for all the signals, while $\mathbf{B}_i$ are different for different signals. This approach enables a two step recovery strategy, where the weights are recovered according to (6) using $\boldsymbol{\Phi}$, while the recovery from $\mathbf{A}_i\mathbf{x}_i$ is formulated as (3).

2.2. Iterative manifold-unaware recovery

Theoretical findings as well as our simulations suggest that the weights estimated using (6) provide good approximation for the original weights using (4). However, we expect that re-computing the weights from the image estimates (specified by (3)), can provide improved estimates, especially at high undersampling factors. Specifically, we propose to alternate between the following steps:

$$\left\{\mathbf{x}_i^{(n)}\right\} = \arg\min_{\mathbf{x}_i} \sum_{i=1}^{k} \|\mathbf{A}_i \mathbf{x}_i - \mathbf{y}_i\|^2 + \lambda\, \mathbf{X}^T \mathbf{L}^{(n-1)} \mathbf{X} \tag{8}$$

$$\mathbf{W}_{i,j}^{(n)} = \varphi\left(\|\mathbf{x}_i^{(n)} - \mathbf{x}_j^{(n)}\| \right), \tag{9}$$

where $\mathbf{x}_i^{(n)}; i = 1, .., k$ are the signals at the n^{th} iteration and $\mathbf{W}^{(n)}$ and $\mathbf{L}^{(n)}$ are the weight matrix and the Laplacian matrix at the n^{th} iteration, respectively. Inspired by half-quadratic regularization schemes in image processing [4, 5, 6], we have shown in [7] that this alternating approach can be seen as a specific majorize minimize algorithm to solve:

$$\{\mathbf{x}_i^*\} = \arg\min_{\{\mathbf{x}_i\}} \sum_i \|\mathbf{A}_i\mathbf{x}_i - \mathbf{y}_i\|_2^2 + \lambda \sum_i \sum_j \phi(\|\mathbf{x}_i - \mathbf{x}_j\|_2), \tag{10}$$

where $\varphi(x) = \phi'(x)/(2x)$.

In this work, we choose the distance function as the truncated ℓ_1 penalty

$$\phi(x) = \begin{cases} 2\sqrt{\epsilon}\sqrt{\|x\|_2^2 + \epsilon} & \text{if} \quad \|x_i\|_2^2 < t \\ 2\sqrt{t\epsilon + \epsilon^2} & \text{else.} \end{cases} \tag{11}$$

Here t and ϵ are constants. With this model, the weights are specified by

$$\mathbf{W}_{i,j}^{(n)} = \begin{cases} \frac{\sqrt{\epsilon}}{\sqrt{\|x_i^{(n)} - x_j^{(n)}\|_2^2 + \epsilon}} & \text{if} \quad \|x_i^{(n)} - x_j^{(n)}\|_2^2 < t \\ 0 & \text{else .} \end{cases} \tag{12}$$

We introduce the threshold t because we want to penalize large distances between vectors less heavily than small distances. Note that the widely used truncated Gaussian weight functions also have similar saturating behavior. The factor ϵ ensures that ϕ is differentiable and $\mathbf{W}_{i,i}$=1. Since the cost function specified by (10) is non-convex, the alternating algorithm specified by (8) and (9) is not guaranteed to converge to the minimum of (10). We propose to use the continuation schemes introduced in [7] to improve the convergence properties. The reformulation of the joint recovery scheme as an optimization scheme enables us to initialize the algorithm with arbitrary weights. Specifically, we propose to compute the weights obtained from a simple scheme (e.g. zero filled or temporal total variation recovery) to initialize the algorithm. Hence, this method can also work with arbitrary sampling patterns.

3. RESULTS

3.1. Simulation results

We use the Physiologically Improved Non uniform CArdiac Torso (PINCAT) phantom [8] to generate a movie of the beating heart in the short axis view, assuming both cardiac and respiratory motion. See a specific frame of the movie and the temporal profile of a row in Fig. 3.(a) and (g). The ratio of the duration of the respiratory to the cardiac cycle is fixed at 4.7. Each image is of size 128x128 and we create a data-set of 600 frames which corresponds to roughly 35 cardiac cycles and 7 respiratory cycles. These movies are undersampled using a variable density random sampling pattern in the Fourier domain. The sampling mask has higher sampling density in the centre of k-space and the density decreases as we move into outer kspace.

We first determine the accuracy of the weights estimated from undersampled data using (6). The Fourier transform of each image in the time series is measured on the same set of locations. The relative error between the weights computed from fully sampled data and the ones obtained from undersampled data are plotted in Fig. 1. These comparisons show that local distances on the manifold can be reliably recovered from approximately 5-7% kspace samples of the data.

We consider the recovery by the proposed two-step and iterative methods in Fig. 3. We use the sampling pattern described by (7), which is illustrated in Fig. 3.(b) and (h). The sampling pattern at each frame is chosen randomly using a variable density mask. We set the undersampling factor to be 6.67; only 15% of the Fourier samples are retained in each frame. A fraction of these samples (corresponding to Φ in (7)) are assumed to be at the same locations for all the frames, while the rest are chosen at random locations. The zero filled IFFT reconstruction are shown in Fig. 3.(c) and (i).

Fig. 3.(d) & (j) show the reconstructions when the sampling pattern is assumed to be same in every frame. Specifically, we set $\mathbf{A}_i = \mathbf{\Phi}; \forall i$. The recovery of the weights is highly accurate since we are retaining 15% of the samples; see from Fig. 1 that only 7% is sufficient to yield accurate weights in this example. However, the lack of diversity between the sampling patterns results in poor reconstruction performance.

We consider the sampling pattern specified by (7), where 7% of the samples are the same locations across frames. The rest (8% of samples) are chosen at random locations. The diversity in the sampling patterns is observed to provide better reconstructions in Fig. 3.(e) and (k). The iterative scheme further improves the results, as seen from Fig. 2.

3.2. Experimental results

We test the iterative recovery algorithm on a cardiac data-set from a 3T MR scanner (Siemens, Trio). The data was acquired using 12 coils in the short-axis view using a steady state free precession radial sequence. We use the golden angle ordering of the rays, where the angle between two consecutive rays is 111.25°. We use 9000 acquired lines to re-

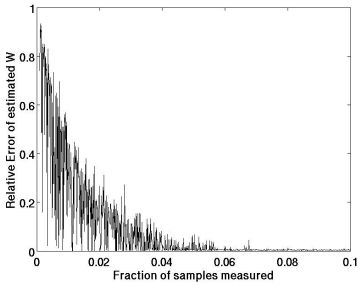

Fig. 1: Accuracy of weight estimation by (6): We plot the normalized error between the weights estimated from fully sampled data and under sampled data using (6) as a function of the fraction of kspace samples measured. The recovery is accurate for greater than 7% measured Fourier samples

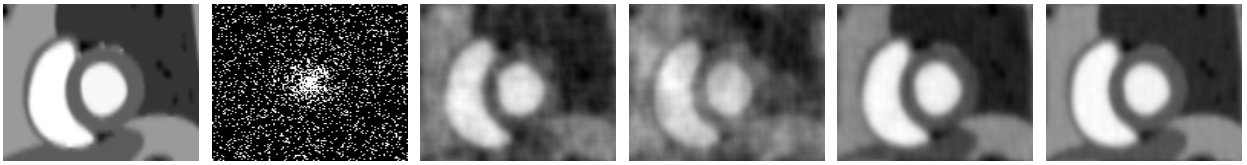

(a) Ground truth (b) Samp. mask: kx-ky (c) Zero filled IFFT (17.03dB) (d) 2 step: $\mathbf{A}_i = \Phi$ (15.10dB) (e) 2 step: $\mathbf{A}_i = (\Phi; \mathbf{B}_i)$(21.02dB) (f) Iterative: $\mathbf{A}_i = \mathbf{B}_i$ (23.32dB)

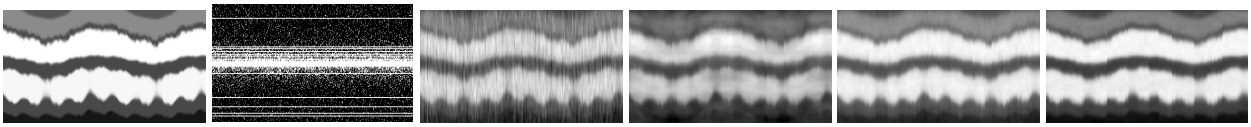

(g) Ground truth (h) Samp. mask: kx-t (i) Zero filled IFFT (j) 2 step: $\mathbf{A}_i = \Phi$ (k) 2 step: $\mathbf{A}_i = (\Phi; \mathbf{B}_i)$ (l) Iterative: $\mathbf{A}_i = \mathbf{B}_i$

Fig. 3: Validation of algorithms on PINCAT free breathing phantom. (a),(c)-(f) Specific image in the time series and its reconstruction (g),(i)-(l) Time profile of a specific row of the image series. (a)&(g) Ground-truth(b)&(h) Mask used to sample Fourier data. A fraction of the samples are acquired at the same locations for all the frames, which is required for the two step approach. (c) Zero-filled IFFT recovery (d) 2-step scheme with with the same sampling masks for all the frames ($\mathbf{A}_i = \mathbf{\Phi}$) (e) 2-step scheme with sampling masks chosen according to (7). Some of the sample locations in each frame are the same across the frames, while the rest are chosen randomly. (f) Iterative scheme, with different random sampling pattern at each frame.

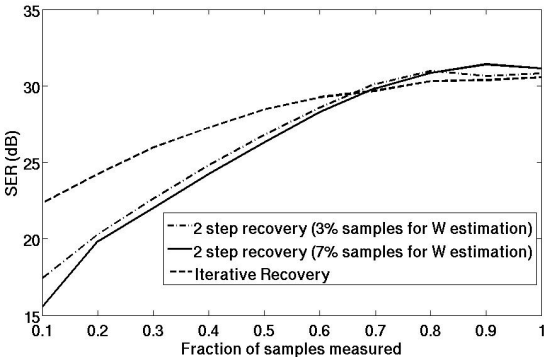

Fig. 2: Accuracy of reconstruction algorithms: We plot the signal to error ratio of reconstructions as a function of the fraction of total kspace samples measured per frame. 2 plots for the 2-step strategy are shown with 3% and 7% respectively of the samples per frame measured at common locations for recovery of W. Iterative strategy is also shown which has no samples at common locations every frame.

construct 600 frames, which corresponds to a temporal resolution of approximately 45 ms. The gridding reconstruction is shown in Fig. 4.(a)&(c). Note that the two step method cannot be used in this case since we do not acquire the samples at the same location in each frame. The reconstruction using the iterative scheme is shown in Fig.4.(b)&(d). This experiment shows that good recovery of a free breathing CINE MRI dataset can be obtained using the proposed scheme.

4. CONCLUSION

We introduced two novel algorithms for the joint recovery of several signals that live on a smooth manifold. The joint recovery scheme only requires the information of local distance distributions on the manifold to obtain the associated graph Laplacian, which is estimated from the under sampled data itself. The first algorithm is a two-step method, which estimates the Laplacian from similar under sampled measurements on all the signals; the Laplacian is then used to recover the signals. Since the second scheme alternates between the estimation of Laplacian and signal recovery, it can be used for arbitrary sampling patterns. We observe that our iterative scheme works well and outperforms the two-step approach for high under-sampling factors. We conclude that for our reconstruction scheme, it is beneficial to sample signals lying on a manifold using incoherent sampling masks since it results in better recovery. Our work results in a simple but efficient alternative to breath-held cardiac MRI.

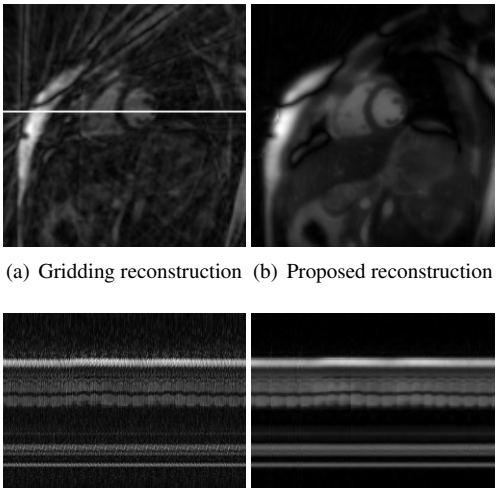

(a) Gridding reconstruction (b) Proposed reconstruction

(c) Gridding reconstruction (d) Proposed reconstruction

Fig. 4: Validation of iterative algorithm on experimental data (a) & (b)A specific image in the time series, recovered using gridding reconstruction and the proposed iterative scheme respectively. (c) & (d) Time profiles of the above images along line shown in (a). Since the data is acquired using golden-ratio patterns, two step schemes cannot be used for the recovery.

5. REFERENCES

[1] Noel C.F. Codella Thanh D. Nguyen Martin R. Prince Jing Liu, Pascal Spincemaille and Yi Wang, "Respiratory and cardiac self-gated free-breathing cardiac cine imaging with multi-echo 3d hybrid radial ssfp acquisition," *Magnectic Resonance in Medicine*, vol. 63, pp. 1230–1237, 2010.

[2] Michael B. Wakin, "Manifold-based signal recovery and parameter estimation from compressive measurements," *arXiv:1002.1247*.

[3] Gabriel Peyre, "Manifold models for signals and images," *Computer Vision and Image Understanding*, vol. 113, pp. 249–260, 2009.

[4] Gilles Aubert Pierre Charbonnier, Laure Blanc-Feraud and Michel Barlaud, "Deterministic edge-preserving regularization in computed imaging," *IEEE Transanctions on Image Processing*, vol. 2, February 1997.

[5] A. H. Delaney and Y. Bresler, "Globally convergent edge-preserving regularized reconstruction: an application to limited-angle tomography," *IEEE Transanctions on Image Processing*, pp. 204–221, February 1998.

[6] Mila Nikolova and Michael K Ng, "Analysis of half-quadratic minimization methods for signal and image recovery," *SIAM Journal on Scientific computing*, vol. 27, pp. 937–966, 2005.

[7] Zhili Yang and Mathews Jacob, "Nonlocal regularization of inverse problems: a unified variational framework," *IEEE Transanctions on Image Processing*, vol. 22, pp. 3192–3203, August 2013.

[8] B. Sharif and Y. Bresler, "Physiologically improved ncat phantom (pincat) enables in-silico study of the effects of beat-to-beat variability on cardiac mr," *Proceedings of the Annual Meeting of ISMRM, Berlin*, 2007.